Check for updates

Environmental DNA metabarcoding of foraminifera for biological monitoring of bottom water and sediments on the Takuyo-Daigo Seamount in the northwestern Pacific

Ayumi Maeda[1]*, Miyuki Nishijima[1], Akira Iguchi[1,2], Yuki Ota[3], Masahiro Suzumura[3] and Atsushi Suzuki[1,2]

[1]Geological Survey of Japan, National Institute of Advanced Industrial Science and Technology (AIST), Tsukuba, Japan, [2]Research Laboratory on Environmentally-Conscious Developments and Technologies (E-code), National Institute of Advanced Industrial Science and Technology, Tsukuba, Japan, [3]Environmental Management Research Institute, National Institute of Advanced Industrial Science and Technology (AIST), Tsukuba, Japan

Foraminifera are adapted to a wide range of environments, and environmental DNA (eDNA) metabarcoding of foraminifera should facilitate development of new environmental indicators. In this study, we used eDNA metabarcoding to evaluate the discrepancy between planktic and benthic foraminifera molecular communities identified in bottom water and short sediment cores. The molecular community was compared to foraminiferal shells in sediment traps set on the seafloor. Samples were collected in June and August around the Takuyo-Daigo Seamount in the western subtropical Pacific Ocean. Approximately 40% of amplicon sequence variants (ASVs) pertained to unknown foraminiferal lineages in sediment samples, compared with only 22% in bottom water. Bottom water contained benthic foraminifera and taxonomically unassigned lineages, which were attributed to resuspended particles. In bottom water, 100 ASVs were assigned to planktic foraminifera. ASVs assigned to *Candeina nitida* were most abundant and accounted for 36%–86% of planktic foraminiferal ASVs. In sedimentary DNA, *Globigerinita glutinata* was the most abundant among 33 ASVs of planktic foraminifera. However, transparent shells in sediment traps contained more spinose species, such as *Globigerinoides ruber*, whereas *C. nitida* was not found and few *G. glutinata* were detected. This discrepancy between the three samples may be due to the species-specific preservation, to polymerase chain reaction biases, and/or to low abundance of planktic foraminifers. In sedimentary DNA, 893 ASVs were assigned to high-level foraminiferal taxa. Among benthic foraminiferal lineages, monothalamids were most abundant, as reported in other deep-sea regions. Molecular communities formed one cluster above the boundary at which ASVs sharply decrease across the three cores. Our results suggest that depth within the sediment core can affect foraminiferal ASVs, but the distance between sites up to 200 m did not strongly affect ASVs of sedimentary DNA at least above the boundary at which ASVs sharply decrease. Sequences of foraminiferal DNA in

sediment decreased linearly in core PC02-A1, but exponentially in core PC03-B3. The decline of foraminiferal ASVs may reflect both the decreases in numbers of living foraminifera and degradation of DNA in sediment, related to the particle mixing depth.

1 Introduction

Deep-sea biological communities support fundamental biogeochemical cycles contributing to ocean stability. With increased interest in commercial mining of deep-sea mineral resources such as polymetallic nodules, polymetallic massive sulfide deposits, and cobalt-rich ferromanganese crusts, deep-sea ecosystems are being investigated to evaluate potential environmental impacts from mineral mining (Gollner et al., 2017; Orcutt et al., 2020). Benthic foraminifera contribute significantly to carbon cycling in the deep sea and are estimated to account for more than 50% of meiofaunal and macrofaunal abundance and biomass on abyssal plains (Gooday et al., 1992; Moodley et al., 2002; Enge et al., 2011). Because benthic foraminiferal assemblages are susceptible to environmental changes, such as food supplies and dissolved oxygen concentrations, in addition to anthropogenic pollutants (Jorissen et al., 1995; Geslin et al., 2004; Duffield et al., 2014), they are used to monitor benthic environmental health (Dimiza et al., 2016; Bouchet et al., 2018). In addition to conventional shell-counting and chemical composition measurements of calcareous tests, high-throughput sequencing (HTS) metabarcoding of environmental DNA (eDNA) for foraminifera has been recently applied to bioassessment and biomonitoring associated with fish farming, oil drilling, and gas platforms (Pawlowski et al., 2014; Laroche et al., 2016; Frontalini et al., 2020). eDNA metabarcoding revealed the dominance of agglutinated and thecate foraminifera (Laroche et al., 2018; Lejzerowicz et al., 2021), expanding morpho-taxonomic data (Cordier et al., 2017). Moreover, benthic foraminifera have been identified as a target to evaluate meiofaunal community structure, using morphological and molecular biological methods recommended by the International Seabed Authority (ISA), the regulating body for deep-sea mining (ISA, 2020). The foraminiferal community has been historically investigated in the Clarion-Clipperton Zone (CCZ), a target region for commercial mining of seabed deposits of polymetallic nodules (Gooday et al., 2021).

On the other hand, planktic foraminifera, which live at the ocean surface are important for monitoring surface physico-chemical properties. Changes in test assemblages are related to seasonal fluctuations in sea surface temperature, primary production, and plankton community structure (Storz et al., 2009; Jonkers and Kučera, 2015; Schiebel and Hemleben, 2017; Maeda

et al., 2022). Furthermore, because fluxes of planktic foraminiferal tests account for 23%–56% of the global open-ocean carbonate flux (Schiebel, 2002), their population fluctuations help to reveal the global oceanic carbon flux. Although planktic foraminifera have been used to understand biological and physico-chemical conditions, modern studies of assemblages using sediment traps and plankton nets are laborious and ineffective. HTS metabarcoding of eDNA targeting planktic foraminifera in seawater may effectively and comprehensively describe community structure using only seawater samples. Seawater samples with eDNA metabarcoding analyses were used to detect microbial and meio- and macro-faunal communities in a previous study (Laroche et al., 2020). However, to the best of our knowledge, there have been no such studies for foraminifera in seawater to date. In addition, the taphonomy of DNA of planktic foraminifera is important to trace assemblages of planktic foraminifera using eDNA. To compare test assemblages, eDNA of bottom water and of sediments help us to understand the potential of eDNA preservation of planktic foraminifera, which can be species specific.

Seamounts have heterogeneous, vulnerable ecosystems (Watling and Auster, 2021), and information about their biological connectivity and biodiversity is still limited (Kvile et al., 2014; Shi et al., 2020). Meanwhile, seamounts attract substantial interest for commercial mining of seabed mineral resources (Nozaki et al., 2016; Toro et al., 2022). Baseline studies, which are necessary for deep-sea mineral mining, are useful for evaluating natural fluctuations of biological communities (Gooday et al., 2017; Jones et al., 2017; Iguchi et al., 2020). In areas covered by solid substrata in the deep sea, such as the summit of the Takuyo-Daigo Seamount (Usui et al., 2017), eDNA metabarcoding using sediment is the first step to understanding existing benthic biological communities containing tiny and rare species (Pawlowski et al., 2022). The aims of this study were (1) to document differences in planktic foraminiferal assemblages between bottom water, sediments, and sediment traps at the seafloor using eDNA metabarcoding analyses, and (2) to identify factors affecting foraminiferal community composition in sediments and bottom water. Variation between shells in sediment traps and molecular communities in bottom water and sediments allow us to understand limitations of detecting DNA of descending foraminiferal tests. We conducted HTS metabarcoding analyses targeting planktic and benthic foraminifers of bottom water and sediment samples collected in June and August at about 940-m depth. Then, molecular

community composition was compared in relation to the collection site, timing, and sediment layer depth.

2 Materials and methods

2.1 Collection of samples

Sediment and bottom water samples were collected repeatedly around a station (water depth ~940 m) on the summit of Takuyo-Daigo Seamount (23°23′N, 153°04′E) in the northwestern Pacific Ocean during cruises of R/V Shinsei-maru in June (cruise JS20-1) and August (JS20-2) 2020 and August 2021 (JS21) (Figure 1). All sediment cores were collected using a push-corer and a remotely operated vehicle (ROV) (Table 1). In June 2020, a sediment core, PC02-A1 was collected from the summit of the seamount (station [St.] PC02, 941-m depth). In August 2020, two sediment cores were collected. One sediment core, PC02-B1 was collected at St. PC02-2 (941-m depth), approximately 5 m from the location of St. PC02. The other sediment core, PC03-B3 was collected at St. PC03 (940-m depth), approximately 200 m from St. PC02. Cores PC02-A1 and PC03-B3 were respectively collected at the same locations as cores TK05-PC02 and TK05-PC03, for age dating, as reported by Ota et al. (2022). Sediment cores were cut horizontally to yield two 0.5-cm slices at the top and then seven 1-cm slices below. These were preserved at −80°C. Bottom water samples were collected using Niskin bottle samplers manipulated by the ROV approximately 3 m above the seafloor in June and August 2020 and August 2021 (Table 2). St. WS-02 and St. WS-03 were collected approximately 200 m from St. WS-01 and St. SW was approximately 600 m from St. WS-01. 1–3-L bottom water samples were filtered onboard using Sterivex filters (0.22-µm mesh, Merck KGaA, Darmstadt, Germany) and the filters were kept at −20°C until DNA extraction. Negative controls with Milli-Q water were prepared in the same way as the bottom water samples. Two sediment traps (SMD13S 6000, NiGK corporation, Kawagoe, Japan) were set on the seafloor at stations St. 3 (938-m depth) and St. 7 (937-m depth). Horizontal distances between St. 3 and PC02 and between St. 7 and PC03 were within 100 m. To prevent degradation of organic materials, cups were preserved with formaldehyde. Time intervals between collections from the two sediment traps are given in Table 3. We used two samples (1 and 13 from ST3 and ST7) to collect sinking particles for 14 days. All sampling sites in this study were within an area 300 m × 300 m square.

2.2 DNA extraction, amplicon library preparation, and sequencing

For sedimentary DNA, we used the 0- to 0.5-cm and 0.5- to 1-cm layers in core PC02-B1 in addition to other 1-cm slices down to a maximum of 8 cm in core PC02-A1 and to 6 cm in core PC03-B3 (Table 1). eDNA was extracted from sediment samples of approximately 5 g from each layer using a Power Max Soil DNA Isolation kit (Qiagen, Hilden, Germany) following the manufacturer's instructions with minor modifications. eDNA was extracted from bottom water samples on Sterivex filters using a DNeasy PowerWater Sterivex kit (Qiagen, Hilden, Germany) according to the manufacturer's instructions. The foraminifer-specific hyper-variable region in the small subunit ribosomal RNA gene (18S rRNA gene) was amplified using forward primer s14F3 (ACGCAMGTGTGAAACTTG; Holzmann et al., 2001) and reverse primer s17 (CGGTCACGTTCGTTGC) with adaptor sequences. polymerase chain reaction (PCR) amplification was performed using 1 µL of template DNA (1 ng µL^{-1}) in a 20-µL reaction volume with Ex Taq polymerase (TaKaRa Bio, Kusatsu, Japan). The first PCR amplification was carried out with the following conditions: a denaturation step at 94°C for 1.5 min; 25 thermal cycles of 1 min at 94°C, 1 min at 50°C, and 1 min at 72°C; 15 cycles of 30 s at 94°C and 30 s at 50°C; and a final extension step at 72°C for 5 min. Triplicates of the first PCR amplicons were mixed to minimize intra-sample variance. All PCR reactions included negative controls with ultrapure water. PCR products were qualitatively checked using a 2% agarose gel, and the target fragment was purified using an Agencourt AMPure XP Kit (Beckman Coulter, Brea, USA) following the manufacturer's protocol. The second PCR was conducted using 1 µL of PCR product in a 20-µL reaction volume with the following
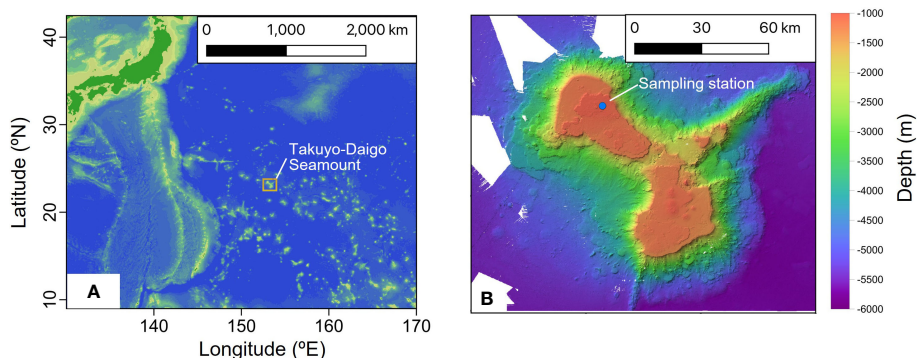

FIGURE 1
(A) Location of Takuyo-Daigo Seamount in the northwestern Pacific and **(B)** sampling station for bottom water, sediment, and sediment trap samples.

TABLE 1 Information about sediment samples used in this study.

Sample ID	Layer (cm)	Site	Date	Depth (m)
PC02-A1_J_0	0–0.5	St. PC02	2020/6/18	941
PC02-A1_J_0.5	0.5–1			
PC02-A1_J_1	1.0–2.0			
PC02-A1_J_2	2.0–3.0			
PC02-A1_J_3	3.0–4.0			
PC02-A1_J_4	4.0–5.0			
PC02-A1_J_5	5.0–6.0			
PC02-A1_J_6	6.0–7.0			
PC02-A1_J_7	7.0–8.0			
PC02-B1_A_0	0–0.5	St. PC02-2	2020/8/18	941
PC02-B1_A_0.5	0.5–1			
PC03-B3_A_0	0–0.5	St. PC03	2020/8/18	940
PC03-B3_A_0.5	0.5–1			
PC03-B3_A_1	1.0–2.0			
PC03-B3_A_2	2.0–3.0			
PC03-B3_A_3	3.0–4.0			
PC03-B3_A_4	4.0–5.0			
PC03-B3_A_5	5.0–6.0			

"J" and "A" in sample IDs represent collection months of June and August.

TABLE 2 Information about bottom water samples used in this study.

Sample ID	Site	Date	Volume (L)	Depth (m)	Sampling depth (m)
JS20-1_J_1	St. WS-01	2020/6/14	1	934	3.1
JS20-1_J_2	St. WS-01	2020/6/15	1	934	1.5
JS20-1_J_3	St. WS-01	2020/6/16	1	934	1.6
JS20-1_J_4	St. WS-01	2020/6/17	1	933	3
JS20-1_J_5	St. WS-01	2020/6/19	1	934	1.5
JS20-1_J_6[*1]	St. WS-01	2020/6/20	1	934	3
JS20-1_J_7[*1]	St. WS-01	2020/6/20	2.35	934	3
JS20-2_A_1	St. WS-01	2020/8/8	1	935	3
JS20-2_A_2[*2]	St. WS-01	2020/8/9	1	940	3
JS20-2_A_3[*2]	St. WS-01	2020/8/9	3		
JS20-2_A_4	St. WS-01	2020/8/15	1	934	1.4
JS20-2_A_5	St. WS-02	2020/8/16	1	942	1.6
JS20-2_A_6	St. WS-03	2020/8/17	1	939	3.3
JS20-2_A_7	St. SW	2020/8/20	1	935	3.1
JS21_A_1	St. WS-01	2021/8/8	2	932.5	1.6

[*1]Samples, JS20-1_J_6 and JS20-1_J_7, were collected during the same ROV dive, but the Niskin bottles and filtering volumes were different.
[*2]Samples of JS20-2_A_2 and JS20-2_A_3 were from the same Niskin bottler, but their filtering volumes were different.

TABLE 3 Information about sediment trap samples used in this study.

Sample ID	Site	Start date	End date	Depth (m)
ST3-1	St.3	2020/6/23	2020/7/7	938
ST3-13	St.3	2020/6/23	2020/7/7	938
ST7-1	St.7	2020/7/18	2020/8/1	937
ST7-13	St.7	2020/7/18	2020/8/1	937

Sediment traps were set on the seafloor.

conditions: initial denaturation for 1 min at 96°C; 15 cycles of 30 s at 96°C, 45 s at 65°C, and 1 min at 72°C; and final extension for 7 min at 72°C. After purification with AMPure XP beads, products from the second PCR were quantified using a Qubit dsDNA HS assay kit with a Qubit 4.0 Fluorometer (Thermo Fisher Scientific, Waltham, USA). We then diluted all quantified index PCR products to the same concentration and prepared one metabarcoding library. We subsequently performed paired-end sequencing (2 × 300 bp) using a MiSeq sequencer (Illumina, San Diego, CA, USA) using a MiSeq Reagent Kit V3 (Illumina) according to the manufacturer's protocol. Raw data from these assays were submitted to the DNA database of Japan (DDBJ) and are available under accession number DRA016254.

Raw FASTQ files were analyzed using the QIIME2 platform (version 2022-02; Bolyen et al., 2019). Low-quality reads (QV < 20) were filtered out, and chimeric reads were identified using "dada2" and removed. Reads were clustered into amplicon sequence variants (ASVs) at complete similarity against the reference database SILVA 138 (https://www.arb-silva.de/documentation/release-138/) and sequences that were not assigned to foraminifera, for example, Archaea, Bacteria, and other Eukaryota were removed for downstream analysis. Although SILVA 138 is a quality-controlled database of small-subunit rRNA genes for bacteria, Archaea, and eukaryotes (Quast et al., 2013), the foraminiferal 18S rRNA data it contains are of insufficient quality and quantity. For this reason, representative sequences of each ASV were then aligned against the National Center for Biotechnology Information (NCBI) nucleotide database according to BLAST+ (Camacho et al., 2009). Only sequences that were assigned to foraminifera (identity rate >92%) and longer alignment length (>200 bp) with more than 10 reads were used for later statistical analysis.

2.3 Microscopic analysis of sediment trap samples at the seafloor

Sediment trap samples ranging from 0.45 μm to 1 mm were filtered and separated into 10 aliquots using a rotary splitter. Total fluxes of sinking particles were calculated by weighing dry samples using five aliquots. For counting shells of foraminifera, we used one aliquot of 1 and 13 of ST3 and ST7, respectively (Table 3). Sinking particles were wet-sieved to 63 μm and foraminiferal shells in >125-μm fractions were picked and counted. We treated (1) broken

shells, (2) pigmented, opaque, or dirty shells as resuspended shells. We recorded transparent shells as newly sinking shells at collection intervals and identified the species following Schiebel and Hemleben (2017).

2.4 Statistical analysis

Coverage-based rarefaction was applied to raw read numbers per ASV (Chao and Jost, 2012) using the "vegan" package (v. 2.6-4; Oksanen et al., 2022) in R (R Core Team, 2021). Subsequently, data were converted to presence/absence data, because foraminifera show various gene copy numbers among and within taxa (Weber and Pawlowski, 2013; Milivojević et al., 2021).

We conducted non-metric multidimensional scaling (nMDS) for the binary eDNA dataset based on Chao distances (Chao et al., 2014) using "vegan" (v. 2.6-4; Oksanen et al., 2022) with the K-medoids clustering method ("cluster" v. 2.1.3; Maechler et al., 2022) to evaluate the similarity of molecular foraminiferal communities between samples of sediment and bottom water. For rarefied abundance data of sediment samples, nMDS was performed based on the Horn-Morisita index. nMDS results were described using "ggplot2" package (Wickham, 2016). Indicator species in each sample based on indicator values were calculated using the "labdsv" package (v. 2.0-1; Roberts, 2019). To evaluate differences in the proportion of the dominant planktic species in bottom water samples, the Wilcoxon rank sum test was conducted between JS20-1 and JS20-2 samples using "exactRankTests" package (v. 0.8-35; Hothorn and Hornik, 2022). We performed permutational multivariate analysis of variance (PERMANOVA) with Chao distances and permutation = 9999 to identify factors affecting differences in molecular community composition for sediment and bottom water samples, respectively. We selected collection month, year, site, depth, and filtered volume as fixed factors for bottom water samples and layer depth, collection site, and month for sediment samples. The layer depth of sediment samples divided into seven groups combining sediment layers deeper than 5 cm into one group as previous molecular studies for foraminifera analyzed up to 5 cm and the ISA guideline recommends that even test assemblages should be studied up to 5 cm (ISA, 2020; Laroche et al., 2020). Best fit models for changes in number of foraminiferal ASVs detected in sediment samples were determined using Akaike's information criterion (AIC). We selected the exponential model

in addition to the linear model because DNA decay rates were often estimated using the exponential model (Jo et al., 2019; Saito and Doi, 2021).

3 Results

3.1 Taxonomic assignment

After quality filtering and removal of the ASVs (<200bp, <92% identity rate) and low-read sequences (≦10), taxonomic assignments were made (Table 4). Bottom water samples yielded a total of 400,616 reads. These contained unidentified foraminifera including sequences obtained from previous environmental foraminiferal metabarcoding analyses (71,437 reads, 83 ASVs) and other sequences (329,179 reads, 258 ASVs) classified to higher taxonomic levels. Globothalamea sequences, including planktic foraminifera, dominated bottom water eDNA samples (Figure 2A). ASVs assigned to benthic and taxonomically unknown lineages showed 17–48 in JS20-1, 9–21 in JS20-2, and 3 in JS21 (Figure 2B). On the other hand, the number of ASVs assigned to planktic foraminifera in each bottom water sample ranged between 6 and 14 in June, 9 and 15 in August, and 100 in total (Table 4; Figure 3). Sequences assigned to *Candeina nitida* dominated planktic foraminifera in bottom water samples (Figure 4). Although *C. nitida* comprised 57%–86% of ASVs in bottom water samples in JS20-1, the proportion of *C. nitida* decreased to 36%–75% in samples from JS20-2 (Supplementary Figure S1, Wilcoxon rank sum test: *p* < 0.05). In bottom water samples from JS21-1, *C. nitida* accounted for 86% and *Globorotalia menardii* accounted for 14% of ASVs. Molecular community datasets between JS20-1, JS20-2, and JS21-1 shared 19,036 reads and 2 ASVs of planktic foraminifera assigned to *C. nitida* and *G. menardii* (Supplementary Figure S2).

In sediment samples, 230,079 reads and 893 ASVs of foraminifera were assigned to taxa above the class level. A total of 151,978 reads constructed 563 ASVs as unidentified foraminiferal sequences in sediment samples. The dominant class-level taxon in almost all sediment samples was Monothalamea (Figure 4A). The number of ASVs in sedimentary DNA clearly decreased with increasing depth in the sediment, from a maximum of 275 at 0.5 cm to 1.0 cm to a minimum of 79 at 7 cm to 8 cm in core PC02-A1, and from a maximum of 239 at 0 cm to 0.5 cm to a minimum of 11 at 4 cm to 5 cm in core PC03-B3 (Table 4; Figure 4B). Four thousand three hundred twenty-nine reads and 33 ASVs were identified as planktic foraminifera in sediment samples, comprising between 0% and 18% of total ASVs in sediment samples. ASVs assigned to *Globigerinita glutinata* were the most abundant in sediment samples.

3.2 Faunal analysis of sediment trap samples at the seafloor

Sediment traps set on the seafloor were the only means for us to count foraminiferal shells to directly compare with molecular data.

Faunal counts of sediment trap samples are shown in Supplementary Table S1. Both ST3-1 and ST7-1 (June–July) exhibited lower total fluxes (47.1 and 23.3 mg m^{-2} d^{-1}) than ST3-13 and ST7-13 (July–August; 107.6 and 39.6 mg m^{-2} d^{-1}). *Globigerinoides ruber*, *Globoturborotalita rubescens*, *Globigerinella siphonifera*, and *G. glutinata* were the abundant species in shell assemblages (Supplementary Table S1). Proportions of resuspended shells and transparent shells of ST3-1 and ST7-1are relatively lower than those of ST3-13 and ST7-13 (Supplementary Table S1). Total transparent shells of sediment trap samples are fewer in number than 50, and no species reached 50% of the assemblages, which is insufficient for statistical analyses of abundance data based on Patterson and Fishbein (1989). Therefore, we converted numbers of shells to presence/absence data to compare the results of planktic foraminifers detected in the molecular community of bottom water and sediments (Table 5).

3.3 Cluster analysis and the best fit model

In bottom water eDNA, cluster analysis visualized with nMDS based on the Chao index showed that molecular communities in JS20-1 separated samples collected at JS20-2 and JS21-1 (Figure 5). Therefore, clusters of bottom water molecular communities may be distinguished by collection month and site. In bottom water samples, indicator sequences were benthic foraminifera for JS20-1 samples, whereas planktic foraminifera sequences were dominant in JS20-2 and JS21 samples (Table 6).

In sediment samples, cluster analysis based on numbers of ASVs indicated that molecular communities in all layers of PC02-A1 and PC02-B1 comprised one cluster with layers <1 cm in PC03-B3. On the other hand, based on abundance data, layers <5 cm in PC02-A1, PC02-B1, and the layers <1 cm in PC03-B3 formed one cluster. Layers >5 cm in PC02-A1 and 1 cm to 2 cm in PC03-B3 comprised another cluster. The rest of PC03-B3 was divided into two clusters. Indicator sequences in sediment samples showed that soft-shelled monothalamids were shared among sites and represented the surface cluster, based on both of the number of ASVs and their abundance (Table 6).

The results of PERMANOVA showed that collection month (R^2 =0.30, P < 0.05), sampling site (R^2 = 0.27, P < 0.001) and sampling year (R^2 = 0.10, P < 0.05) had effects on foraminiferal molecular communities in bottom water samples (Supplementary Table S2). Depth and filtering volume did not significantly influence foraminiferal molecular communities. In sediment samples, foraminiferal molecular communities were influenced by collection month (R^2 = 0.25, P < 0.01) based on the number of ASVs, whereas layer depth (R^2 = 0.43, P < 0.05) and collection month (R^2 = 0.12, P < 0.05) affected molecular communities based on abundance data.

Results of best fit models for changes in numbers of foraminiferal ASVs detected in sediment samples are given in Supplementary Table S3 and in Figure 6. Based on AIC, the best fit model for changes in number of foraminiferal ASVs was a linear model for the core PC02-A1, whereas an exponential decline was described for PC03-B3.

TABLE 4 Summary of taxonomic assignments for (A) bottom water and (B) sediment samples based on amplicon sequence variances.

(A)	Unassigned	Mono	Globo	Tubo	Benthic	Planktic	Total
JS20-1_J_1	5	5	20	0	18	7	30
JS20-1_J_2	13	5	22	0	14	13	40
JS20-1_J_3	9	9	12	0	15	6	30
JS20-1_J_4	11	15	14	2	24	7	42
JS20-1_J_5	7	10	15	0	17	8	32
JS20-1_J_6	2	12	10	0	15	7	24
JS20-1_J_7	13	23	24	2	35	14	62
JS20-2_A_1	5	5	10	0	5	10	20
JS20-2_A_2	7	10	11	0	10	11	28
JS20-2_A_3	6	13	11	0	15	9	30
JS20-2_A_4	5	9	15	0	9	15	29
JS20-2_A_5	10	3	11	0	4	10	24
JS20-2_A_6	6	9	12	0	10	11	27
JS20-2_A_7	5	3	12	0	4	11	20
JS21-1_A_1	0	0	7	0	3	4	7
B	Unassigned	Mono	Globo	Tubo		Nodo	Total
PC02-A1_J_0	101	74	54	7		9	245
PC02-A1_J_0.5	110	83	65	10		7	275
PC02-A1_J_1	79	74	50	6		10	219
PC02-A1_J_2	75	67	41	5		7	195
PC02-A1_J_3	81	61	38	4		6	190
PC02-A1_J_4	78	62	43	2		7	192
PC02-A1_J_5	47	25	23	7		1	103
PC02-A1_J_6	57	38	30	4		4	133
PC02-A1_J_7	39	19	14	6		1	79
PC02-B1_A_0	84	61	57	5		4	211
PC02-B1_A_0.5	75	81	37	7		7	207
PC03-B3_A_0	101	69	62	3		4	239
PC03-B3_A_0.5	76	69	35	2		3	185
PC03-B3_A_1	43	37	19	1		2	102
PC03-B3_A_2	46	40	15	2		1	104
PC03-B3_A_3	27	18	6	3		1	55
PC03-B3_A_4	5	4	2	0		0	11
PC03-B3_A_5	10	12	3	0		0	25

Total number of ASVs means the sum of "Benthic," "Planktic," and "Unassigned" and are equal to sums of "Unassigned," "Mono," "Globo," and "Tubo." Mono, Monothalamea; Globo, Globothalamea; Tubo, Tubothalamea; Nodo, Nodosariata.
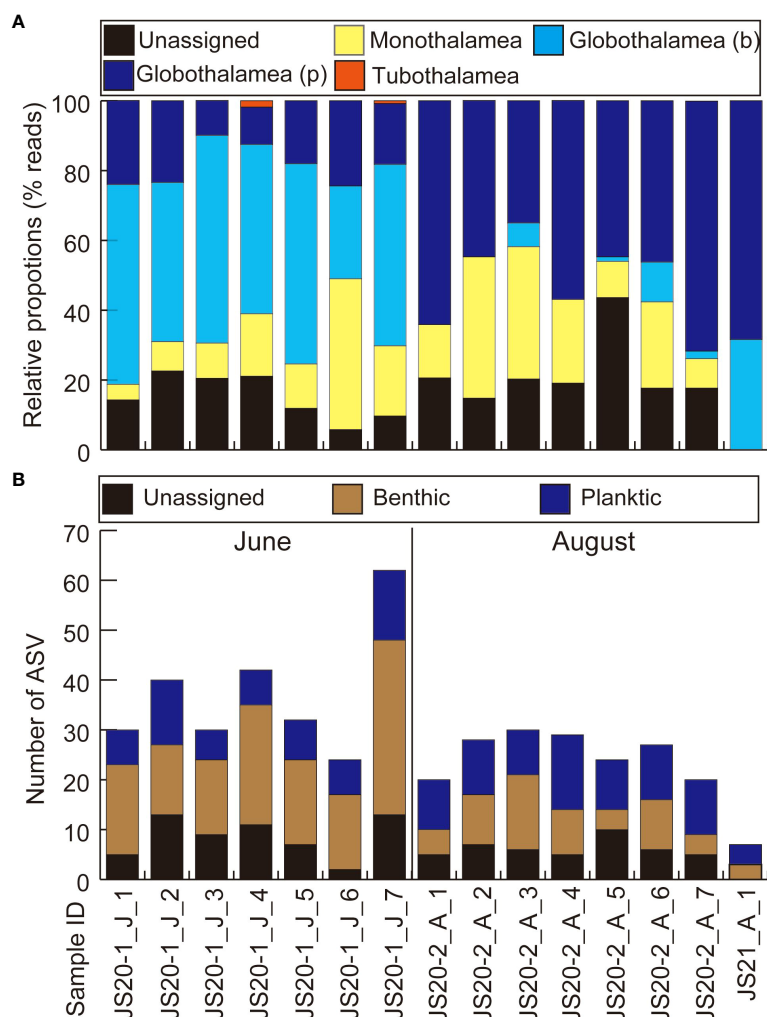
FIGURE 2
Results of eDNA metabarcoding analyses of bottom water **(A)** based on numbers of reads and **(B)** based on numbers of ASVs. **(A)** Globothalamea (b) represents benthic foraminifera belonging to the Class Globothalamea. Globothalamea (p) represents planktic foraminifera belonging to the Class Globothalamea. "J" and "A" in sample IDs represent collection months of June and August.

4 Discussion

4.1 Characteristics of foraminifera detected in bottom water eDNA

In bottom water eDNA, ASVs of planktic foraminifera accounted for more than 50% of most samples in August, whereas benthic ASVs were more abundant than planktic ASVs in June samples (Figure 2). Planktic foraminifera generally dwell between 0-m and 300-m depth, according to previous studies using vertically separated plankton tows (Schiebel, 2002; An et al., 2018; Davis et al., 2021). In this study, in seawater collected within 3 m of the seafloor, planktic foraminiferal sequences would be derived from tests descending from the surface. The settling velocity of planktic foraminiferal tests varies among species (0.03 m s^{-1} to 0.04 m s^{-1} on average; Caromel et al., 2014; Walker et al., 2021), and tests can descend to ~1000 m below the surface within a few days. Because eDNA degradation can be accelerated by enzyme concentrations and microbial activity, and indirectly by high temperature and UV irradiation, and it is difficult

to accurately estimate eDNA decay time (Strickler et al., 2015; Seymour et al., 2018; Jo et al., 2019; Saito and Doi, 2021; Joseph et al., 2022). Although eDNA in water decays more rapidly than in sediment, it persists from several days to several weeks, according to previous studies reporting DNA decay rates of 0.0097–0.101 (Sassoubre et al., 2016; Sansom and Sassoubre, 2017). Therefore, DNA in individual tests could remain in bottom water for at least several days before being completely degraded.

Furthermore, only 17 of 335 total ASVs and 10 in 100 planktic foraminiferal ASVs were shared between bottom water samples collected in the JS20-1 and JS20-2 (Supplementary Figure S2). It is possible that most eDNA detected in bottom water in June could have decayed in August, even though addition of DNA from the same planktic foraminifers still living in August was taken into account. Unlike eDNA in bottom water samples, eDNA adsorbed to sediment persists longer at year scale, and the fine sediments such as clay more efficiently bind DNA than coarse sands (Joseph et al., 2022). Although we cannot reject the possibility that ancient planktic foraminiferal eDNA was resuspended from sediment by
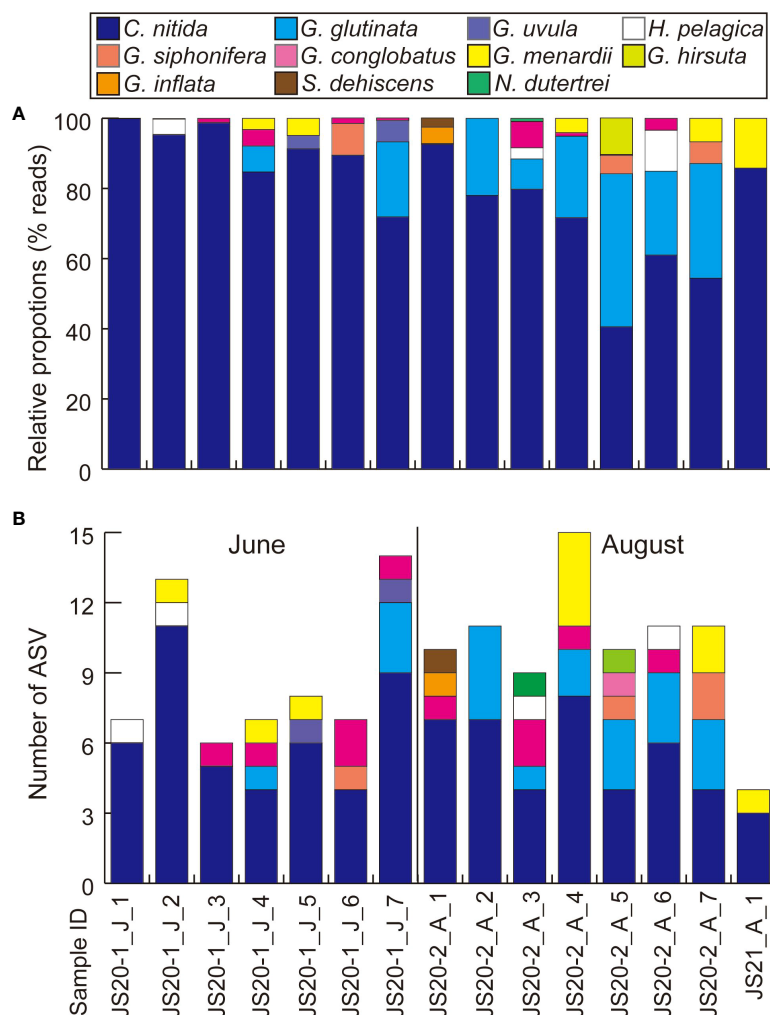
FIGURE 3
Results of eDNA metabarcoding analyses of bottom water focusing on planktic foraminifera **(A)** based on numbers of reads and **(B)** based on numbers of ASVs. "J" and "A" in sample IDs represent collection months of June and August.
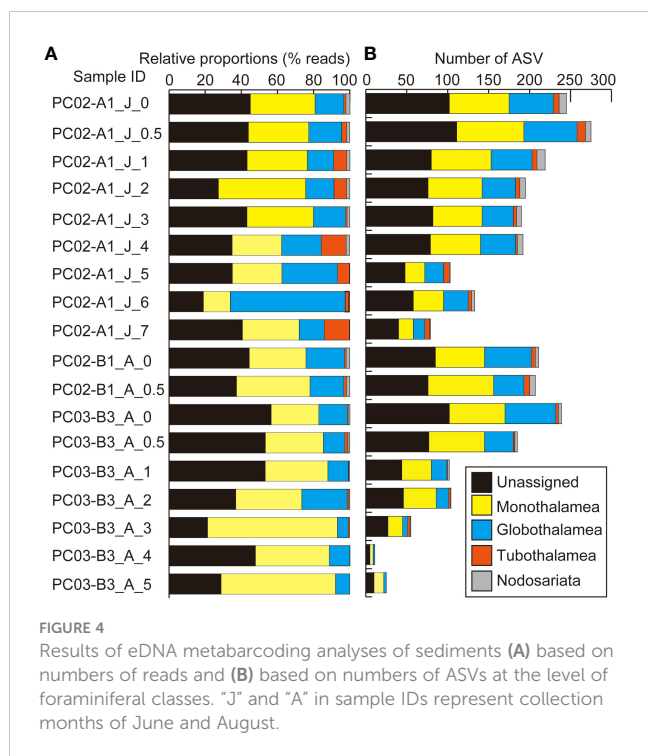
bottom currents or from disturbance by the ROV landing on the bottom, it is unlikely that poorly preserved planktic foraminiferal eDNA (approximately 700 reads at the maximum in a sample) in allochthonous foraminiferal ooze could contribute much to the total eDNA of planktic foraminifera. The influence of contamination of benthic foraminiferal DNA can be high (up to 77% in the number of ASVs) in bottom water samples because of the collection height of ~3 m above the seafloor. Even though sequences of benthic foraminifera influence molecular communities to a certain extent, only ASVs assigned to planktic species showed substantial differences between samples collected in June and August.

4.2 Biased molecular community of planktic foraminifera detected between bottom water and sedimentary eDNA

ASVs assigned to *C. nitida* dominated the planktic foraminiferal community derived from eDNA in all bottom water samples: 57%–86% in June and 36%–75% in August (Figure 3). The dominance of

C. nitida contradicts its rarity in previous sediment-trap and plankton-tow studies worldwide (Bé and Tolderlund, 1971; Lessa et al., 2020; Meilland et al., 2022). Furthermore, *C. nitida* was not found in sediment traps on the seafloor. In spite of the relatively low similarity of sequences assigned to *C. nitida* (less than 95% of 49 ASVs in total 66 ASVs, ≥10 reads), the dendrogram of *C. nitida* ASVs showed that these ASVs belonged to one cluster including *C. nitida* reference sequences and differed from *Tenuitellita fleisheri*, and *T. iota*, belonging to the family Candeinidae (Supplementary Figure S3).

The dominance of *C. nitida* sequences can be caused by (1) reproduction, (2) PCR biases, (3) preservation biases, and (4) the low abundance of planktic foraminifera. Because foraminifera are single-celled organisms, gametogenic individuals (Darling et al., 1996), gametes from sexual reproduction (Weinkauf et al., 2022), and asexually reproduced offspring could be included in eDNA metabarcoding using 18S rDNA. Although gametogenesis releasing gametes in planktic foraminifera has only been rarely observed (Bé and Anderson, 1976), and that of *C. nitida* has never been seen, monthly or semi-monthly cyclic reproduction with large numbers of

FIGURE 4
Results of eDNA metabarcoding analyses of sediments **(A)** based on numbers of reads and **(B)** based on numbers of ASVs at the level of foraminiferal classes. "J" and "A" in sample IDs represent collection months of June and August.

gametes and offspring as observed for other planktic species could partially explain the excessive reads of *C. nitida* (Jonkers et al., 2015). However, the low abundance of *C. nitida* even in the often "ignored" 63 μm to125 μm fraction in a previous sediment trap survey (Chernihovsky et al., 2018) suggest that *C. nitida* releases small numbers of gametes and asexually reproduced offspring, or the rate of maturation would be low. Although lack of knowledge hinders understanding of the reproductive process of *C. nitida*, gametes and offspring cannot account for their dominance in eDNA.

In addition, gene copy numbers vary widely between species of planktic foraminifera (~4000–50,000) and among individuals of the same species (~300–350,000) (Milivojević et al., 2021). Although the gene copy number of *C. nitida* is still undetermined, various orders of gene copy numbers among foraminifera imply that *C. nitida* sequences are likely overestimated by a vast number of gene copies. As reported in Morard et al. (2017), preferential PCR amplification for microperforate species, including Candeinidae and Globigerinitidae in addition to PCR biases that impair dominant Globigerinidae, such as *Trilobatus sacculifer* and *G. ruber*, could skew molecular communities (Barrenechea Angeles et al., 2020). Although sediment traps at the seafloor did not fully reflect surface planktic foraminiferal assemblages, globigerinids,

such as *G. ruber* and *G. rubescens*, are major components (Table 5; Supplementary Table S1). However, globigerinids, except for *G. siphonifera* and *Globigerinoides conglobatus*, could not be detected in bottom water.

Although species-specific DNA preservation might affect molecular community structure, it is hard to assess resistance to DNA degradation due to negative PCR biases for Globigerinidae. Barrenechea Angeles et al. (2020) reported no systematic biases caused by different shell sizes, shapes, and thickness in their sedimentary DNA study in the northwestern Atlantic. In our sedimentary DNA, the dominant planktic sequences originated from *G. glutinata*, whereas *C. nitida* sequences were the second most abundant. In addition, seven ASVs of *C. nitida* were detected in the upper 3 cm of sediment layers, whereas *G. glutinata* was detected down to 6 cm (Supplementary Figure S4). The number of ASVs and the detection limits of sediment layer depth imply that DNA of *C. nitida* does not persist much longer than DNA of *G. glutinata*.

On the other hand, the high proportion of *C. nitida* in June, the presence of planktic indicator species except for *C. nitida* in August samples, and less diverse sequences of planktic foraminifera from bottom water eDNA in June (Figure 3; Supplementary Figure S1; Table 6A) suggest that a minimum in the total flux of planktic foraminifera reinforces the apparent dominance of *C. nitida*. Tropical planktic foraminiferal assemblages show clear seasonal variation of abundance and the interval of minimum abundances depends on the area (e.g., Kawahata et al., 2002; Yamasaki et al., 2008; Chernihovsky et al., 2018; Maeda et al., 2022). The North Pacific Subtropical Gyre is a data-poor region of temporal planktic foraminiferal assemblage (Chaabane et al., 2023). Nevertheless, *G. ruber* and *T. sacculifer* are major components in that assemblage, especially during low abundance from June to August in the tropical equatorial Pacific (Kawahata et al., 2002; Yamasaki et al., 2008). Therefore, the low abundance of planktic foraminifera and low detection of the dominant Globigerinidae using metabarcoding analyses may contribute to biased bottom water molecular communities, rich in *C. nitida* (Figure 3).

Briefly, *C. nitida* was most abundant in aqueous DNA of bottom water and *G. glutinata* was most widely detected in sedimentary DNA, whereas spinose species were plentiful in shells. The discrepancy in dominant planktic foraminifers between the three samples could be caused by preservation biases, species-specific success of PCR, or low abundances of planktic foraminifers. The two clusters of bottom water molecular communities could be distinguished by collection month (PERMANOVA: $R^2 = 0.30$, $P < 0.05$). However, we cannot determine whether seasonality of planktic foraminifera can be investigated using aqueous DNA metabarcoding

TABLE 5 Presence and absence of transparent shells of planktic foraminifers in sediment trap samples set on the seafloor.

	sac	con	rub	rubs	ten	glu	sci	tru	Gt	orb	bul	cal	sip	pel	T	Total
ST3-1 & ST7-1		+	+	+	+	+	+	+		+	+		+		+	11
ST3-13 & ST7-13	+	+	+	+	+	+		+	+	+		+	+	+	+	13

sac: *T. sacculifer*, con: *G. conglobatus*, rub: *G. ruber*, rubs: *G. rubescens*, ten: *G. tenella*, glu: *G. glutinata*, sci: *G. scitula*, tru: *G. truncatulinoides*, Gt: *Globorotalia sp.*, orb: *O. universa*, bul: *G. bulloides*, cal: *G. calida*, sip: *G. siphonifera*, pel: *H. pelagica*, T: *Tenuitella* sp. +: present.
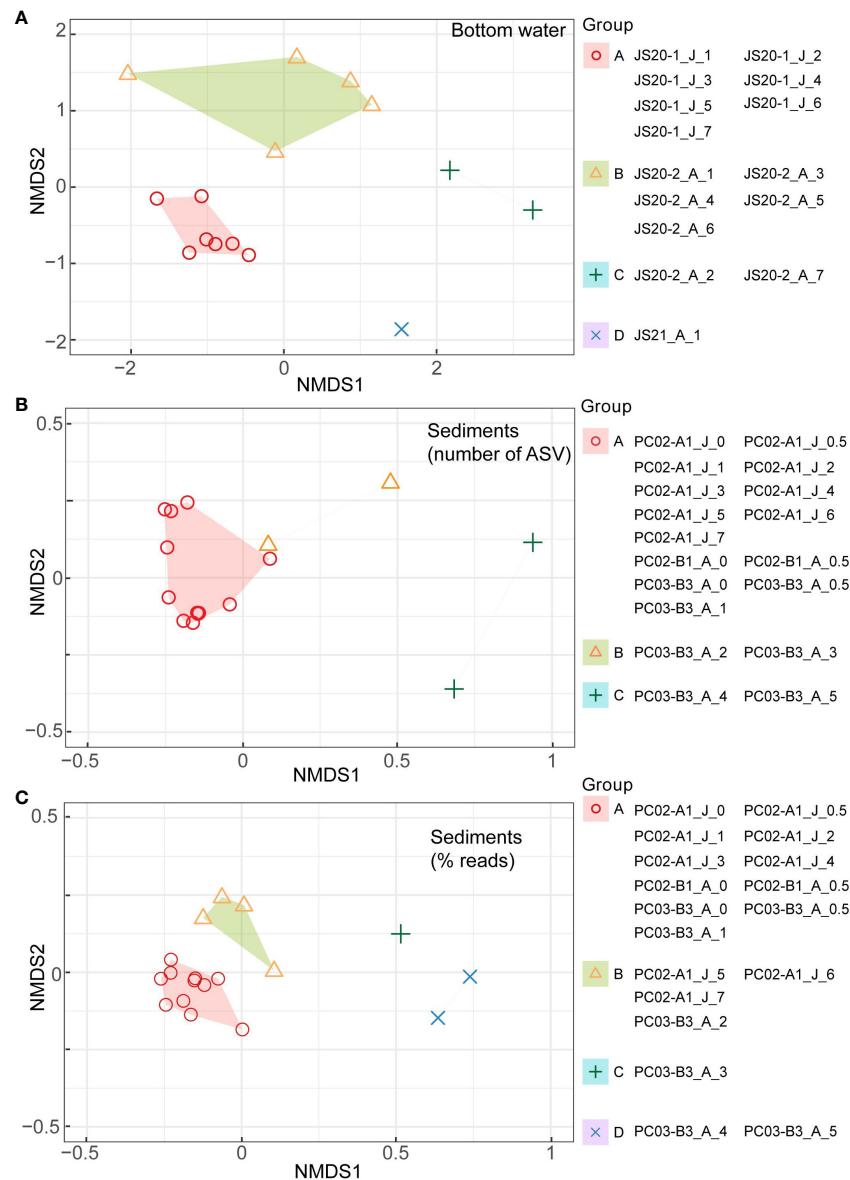
FIGURE 5
Results of cluster analyses of **(A)** bottom water, **(B)** sediment samples based on numbers of ASVs (middle), and **(C)** sediment samples based on rarefied abundance data (lower) visualized in non-metric multidimensional scaling (nMDS) for the binary eDNA dataset based on Chao distances (Chao et al., 2014) and the Horn-Morisita index with K-medoids clustering methods. "J" and "A" in sample IDs represent collection months of June and August. The packages, "vegan," "cluster," and "ggplot2" in R were used.

analyses without a comparison with surface test assemblage of planktic foraminifera. Further studies are required to evaluate biases between foraminiferal molecular and test assemblages and to detect more species (Globigerinidae) effectively.

4.3 Characteristics of foraminifera detected in sedimentary DNA

Unassigned foraminiferal sequences accounted for 37%–51% of sediment samples based on number of ASVs and predominant unassigned foraminiferal sequences were also reported by previous studies in abyssal sediments in CCZ (Lejzerowicz et al., 2021).

Abundant unassigned foraminiferal sequences suggest numerically important new taxa, although poor coverage of the reference database can cause taxonomic assignment failures reported by previous studies (Pawlowski et al., 2014; Lejzerowicz et al., 2021). Monothalamids accounted for 23%–48% of foraminiferal ASVs in sedimentary eDNA, and Globothalamea ASVs were the second most abundant (11%–27%) in this study, comparable to the dominance of monothalamids in sedimentary eDNA reported by previous surveys using deep-sea sediments (Shi et al., 2020; Gooday et al., 2021; Shi et al., 2021).

The result of nMDS based on numbers of ASVs differed from that based on abundance data (Figure 5). Based on the number of ASVs, nMDS included all layers of PC02-A1 in one cluster.

TABLE 6 Summary of indicator species for (A) bottom water, (B) sediment samples based on amplicon sequence variances, and (C) sediment samples based on abundance data.

A group	Indval	*p* value	Freq	Class	Taxonomy	NCBI accession number of best Blast hit	% identity to best Blast hit
A	1	0.001	7	Globo	*Cribrostomoides* sp.	HG425224.1	95.238
A	0.695	0.018	7	Globo	*Cribrostomoides* sp.	HG425224.1	92.353
A	0.584	0.021	8	Unassigned	Uncultured foraminifera	JX297936.1	98.773
A	0.714	0.01	5	Unassigned	Uncultured foraminifera	JX297852.1	92.279
A	0.857	0.006	6	Mono	*Allogromia* sp.	HE998678.1	92.941
B	0.8	0.002	4	Mono	*Crithionina* sp.	AJ307760.1	92.898
B	0.679	0.027	5	Globo	*Globigerinoides conglobatus*	MN384152.1	99.701
C	1	0.01	2	Globo	*Globigerinita glutinata*	HG425205.1	99.102

B group	Indval	*p*-value	Freq	Class	*Taxonomy*	NCBI accession number of best Blast hit	% identity to best Blast hit
A	0.667	0.009	15	Mono	*Monothalamids* sp.	OL873252.1	95.33
A	0.929	0.002	13	Mono	*Allogromiina* sp.	AJ307874.1	96.016
A	0.604	0.019	14	Mono	*Saccamminid* sp.	KP984706.1	94.239
A	0.786	0.014	11	Mono	*Saccamminid* sp.	KP984706.1	92.411
A	0.714	0.024	10	Mono	*Saccamminid* sp.	KP984706.1	94.715
A	0.714	0.026	10	Mono	*Saccamminid* sp.	KP984706.1	95.122
A	0.857	0.007	12	Globo	*Gavelinopsis praegeri*	LN851686.1	92.373
A	0.714	0.018	10	Globo	*Nummulites venosus*	OK415096.1	94.17
A	1	0.001	14	Unassigned	Uncultured foraminifera	JX297861.1	92.72
A	0.604	0.024	14	Unassigned	Uncultured foraminifera	JX297838.1	93.37
A	0.714	0.017	10	Unassigned	Uncultured foraminifera	MW053362.1	95.019
A	0.857	0.005	12	Unassigned	Uncultured foraminifera	JX297864.1	99.717
B	0.519	0.047	15	Mono	*Allogromida* sp. 2	HE998686.1	97.156
B	1	0.015	2	Mono	*Monothalamids* sp.	OL873226.1	95.26
B	1	0.01	2	Globo	*Nonionella labradoricai*	FJ705896.1	92.697
B	1	0.016	2	Tubo	*Siphonaperta* sp.	FR839765.1	92.192
B	0.933	0.044	3	Unassigned	Uncultured foraminifera	JX297856.1	99.148
B	1	0.016	2	Unassigned	Uncultured foraminifera	FJ646679.1	97.586
B	1	0.019	2	Unassigned	Uncultured foraminifera	JX297907.1	94.6

(Continued)

TABLE 6 Continued

B group	Indval	*p*-value	Freq	Class	*Taxonomy*	NCBI accession number of best Blast hit	% identity to best Blast hit
B	1	0.014	2	Unassigned	*Uncultured foraminifera*	JX297867.1	98.86
B	1	0.014	2	Unassigned	*Uncultured foraminifera*	JX298028.1	92.643
B	0.933	0.037	3	Unassigned	*Uncultured foraminifera*	JX298028.1	97.479
B	0.933	0.022	3	Unassigned	*Uncultured foraminifera*	JX297907.1	94.03
C	1	0.013	2	Mono	*Monothalamids* sp.	OL873227.1	94.23
C	0.667	0.033	3	Globo	*Globigerinita glutinata*	HG425205.1	92.478
C Group	**Indval**	***p*-value**	**Freq**	**Class**	***Taxonomy***	**NCBI accession number of best Blast hit**	**% identity to best Blast hit**
A	0.903	0.001	14	Unassigned	*Uncultured foraminifera*	MW053371.1	94.942
A	0.776	0.001	12	Unassigned	*Uncultured foraminifera*	JX298028.1	96.056
A	0.685	0.001	14	Unassigned	*Uncultured foraminifera*	JX297838.1	93.37
A	0.818	0.002	9	Unassigned	*Uncultured foraminifera*	JX297882.1	92.43
A	0.864	0.001	14	Unassigned	*Uncultured foraminifera*	JX297861.1	92.72
A	0.906	0.001	13	Mono	*Allogromiina* sp.	AJ307874.1	96.016
A	0.876	0.021	15	Mono	*Allogromida* sp. 2	HE998686.1	97.156
A	0.891	0.001	11	Mono	*Saccamminid* sp.	KP984706.1	92.411
A	0.967	0.002	12	Mono	*Psammosphaera* sp.	AJ307743.1	98.476
A	0.909	0.002	10	Mono	*Saccamminid* sp.	KP984706.1	94.715
A	0.766	0.044	10	Mono	*Saccamminid* sp.	KP984706.1	95.122
A	0.818	0.001	9	Mono	*Allogromiina* sp.	AJ307874.1	96.016
A	0.818	0.01	9	Mono	*Saccamminid* sp.	KP984706.1	94.094
A	0.833	0.001	12	Mono	*Saccamminid* sp.	KP984706.1	94.538
A	0.727	0.017	8	Mono	*Allogromida* sp. 2	HE998686.1	96.875
A	0.818	0.032	9	Mono	*Syringammina corbicula*	EU672993.1	94.643
A	0.909	0.001	10	Globo	*Nummulites venosus*	OK415096.1	94.17
B	0.729	0.002	15	Mono	*Monothalamids* sp.	OL873252.1	95.33
B	0.813	0.004	7	Mono	*Micrometula* sp.	HE998682.1	95.51
C	0.829	0.019	7	Unassigned	*Uncultured foraminifera*	JX297867.1	96.023
C	1	0.048	1	Unassigned	*Uncultured foraminifera*	JX298028.1	95.775
C	0.857	0.043	3	Unassigned	*Uncultured foraminifera*	JX297907.1	94.03

(Continued)

TABLE 6 Continued

C Group	Indval	*p*-value	Freq	Class	*Taxonomy*	NCBI accession number of best Blast hit	% identity to best Blast hit
C	1	0.043	1	Unassigned	*Uncultured foraminifera*	JX873941.1	92.337
C	1	0.045	1	Unassigned	*Uncultured foraminifera*	JX297856.1	98.4
C	1	0.048	1	Mono	*Monothalamids* sp.	OL873226.1	95.08
C	1	0.044	1	Mono	*Micrometula* sp.	LN873549.1	96.875
C	1	0.048	1	Mono	*Aschemonella* sp. 2	LT796820.1	94.66
C	0.988	0.044	2	Mono	*Pilulina argentea*	OL873225.1	92.74
C	1	0.049	1	Mono	*Allogromiina* sp.	AJ307763.1	93.525
D	1	0.006	2	Mono	*Monothalamids* sp.	OL873227.1	94.23

Group = group in Figure 5, Freq, frequency; Indval, individual value; Mono, Monothalamea; Globo, Globothalamea.

However, nMDS based on abundance data indicated that the boundary layer in which ASVs rapidly decreased in PC02-A1 (5 cm to 6 cm) and PC03-B3 (1 cm to 2 cm) was comparable to cluster boundary layers. Almost all layers above the ASV threshold formed one cluster due to particle mixing (see Section 4.4).

Collection sites of cores influenced sedimentary molecular communities of foraminifera less (PERMANOVA: $R^2 = 0.034$, $P > 0.1$). As molecular analyses of benthic foraminifera showed a low proportion of identical sequences over replicates from the cores (Lejzerowicz et al., 2014), benthic foraminifera are patchily
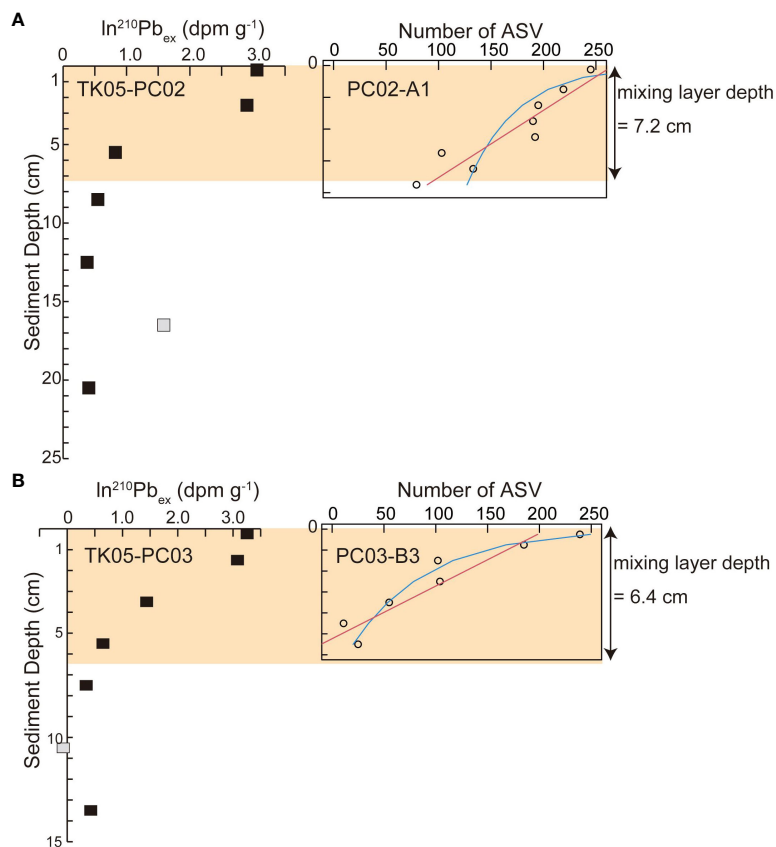

FIGURE 6
Comparison between particle mixing depth estimated based on ln(^{210}Pb) (Ota et al., 2022) and depth profiles of ASVs of foraminifera in **(A)** St. PC02 and **(B)** St. PC03. Red lines represent linear models for decreasing numbers of ASVs of foraminifera, and blue lines represent exponential models for decreasing numbers of ASVs. Gray squares represent eliminated data of ln(^{210}Pb) in Ota et al. (2022).

distributed (Li et al., 2022). However, based on cluster analyses, indicator sequences of the surface cluster, such as Allogromiidae and Saccamminidae, occurred throughout cores and depths (Tables 6B, C). Therefore, a horizontal distance of 200 m has little effect on the benthic foraminifera community, at least in layers above the ASV threshold.

Several ASVs assigned to planktic species (0%–18%) may have been derived from settling tests of planktic foraminifera (Morard et al., 2017; Shi et al., 2021; Cao et al., 2022; Li et al., 2022). Planktic foraminiferal sequences accounted for less than 10% of total sedimentary sequences, which is consistent with previous studies, except for Li et al. (2022), targeting mainly the Rotaliida and Textulariida, (Table S4; Morard et al., 2017; Shi et al., 2021; Cao et al., 2022; Li et al., 2022). Planktic molecular communities in each oceanic area varied, but contained microperforate species including *C. nitida* and *G. glutinata* (Supplementary Table S2), which reflects the cosmopolitan distribution of both species detected using metabarcoding methods targeting planktic foraminifera (Morard et al., 2019).

4.4 Comparison between degradation of DNA of foraminifera and particle mixing depth

The total number of ASVs diminished sharply with depth in the sediment (Figure 4B). Even though several infaunal species can live at sediment depths exceeding 10 cm (Corliss, 1985; Gooday, 1986), previous morphological studies have reported that the abundance and number of species of living benthic foraminifera, especially plano-convex and bi-convex species, rapidly decrease at sediment depths greater than 2 cm to 3 cm, due to the decrease in dissolved oxygen (Corliss, 1985; Geslin et al., 2004). Also, because preserved foraminiferal DNA is increasingly degraded as depth increases (Barrenechea Angeles et al., 2020), the number of ASVs detected declines in deeper layers. Thus, the decrease of ASVs of benthic foraminifera reflects both the decrease in numbers of living individuals and degradation of DNA in sediment.

Deng et al. (2020) noted that bacterial, eukaryotic, and archaean community shifts based on molecular analyses are regulated by dissolved O_2 introduced by bioturbation and organic matter transported by reworking in the mixing layer. Estimated particle mixing depths at St. PC02 (7.2 cm; Ota et al., 2022) and St. PC03 (6.4 cm; Ota et al., 2022) were within the global mean mixing depth of 5.75 cm ± 5.67 cm (± SD, Teal et al., 2008), and heterogenous surface mixing could be attributed to a rise between St. PC02 and St. PC03. Even though the best fit models for foraminiferal ASVs differ between PC02-A1 and PC03-B3 (Figure 6; Supplementary Table S3), the declining trend of foraminiferal ASVs is related to the particle mixing depth (Figure 6). The sampling resolution of eDNA analyses (by 0.5 cm or 1 cm) and radioisotopes (by 2 cm or 3 cm) differ. However, the linear decline of ASVs is comparable to the decline of ^{210}Pb and stable ^{14}C up to 5.5 cm at St. PC02 (Ota et al., 2022), which imply year-scale particle mixing, and gradual decay of DNA and decrease of living foraminifera. The shallow ASV

threshold of around 1 cm in PC03-B3 indicated by exponential decline could be consistent with a well-mixed surface layer indicated by nearly stable ln($^{210}Pb_{ex}$) and ^{14}C ages of TK05-PC03 (Ota et al., 2022), which imply high potential for physical mixing and living foraminifera around 1 cm. Decay processes of foraminiferal DNA and radioisotopes do not yield exactly the same picture. Both datasets exhibit comparable particle mixing conditions, because sedimentary particles are substrates and particle behavior strongly affects both DNA and radioisotopes. Direct correlation of ASV numbers and mixed-layer depth using geochemical signals are not appropriate because estimation processes of ASVs and mixed-layer depth include biases. Nevertheless, Petro et al. (2019) reported that biomasses of bacteria and archaea show consistent trends and thresholds with radioisotopes in the bioturbation zone. Similarly, eDNA metabarcoding data of foraminifera may provide Supplementary Information for particle mixing determined by geochemical tracer data. To confirm the relationship between the molecular community of foraminifera and particle mixing conditions based on geochemical signals, further investigation of processes of degradation for sedimentary DNA and radioisotopes is needed.

5 Conclusions

We investigated planktic and benthic foraminiferal assemblages using eDNA metabarcoding methods in the area covered by allochthonous foraminiferal ooze on the summit of the Takuyo-Daigo Seamount. In bottom water samples, contamination of benthic foraminiferal DNA was attributed to resuspension, as observed in resuspended shells of sediment trap samples. *C. nitida* was most abundant in aqueous DNA of bottom water and *G. glutinata* was most widely detected in sedimentary DNA, while spinose species were plentiful in shells. The discrepancy in dominant planktic foraminifers between the three samples can be caused by preservation biases, species-specific success rate of PCR, and low abundances of planktic foraminifers. Collection timing and sites contributed to differences among samples.

On the other hand, communities of foraminifera identified in eDNA from sediment samples were affected by sediment-layer depth in cores and sampling months. Unassigned foraminiferal and monothalamid sequences were dominant. ASVs of sedimentary DNA decreased linearly as depth increased at St. PC02, whereas ASVs decreased exponentially at St. PC03. Thresholds of numbers of foraminiferal ASVs in sediments were comparable to particle mixing depths determined using radioisotopes.

Data availability statement

The datasets presented in this study can be found in online repositories. The names of the repository/repositories and accession number(s) can be found in the article/Supplementary Material.

Author contributions

AI, AS, and MS designed the study. AS conducted field work and sampling at sea. MN conducted experiments and MN and AM performed analyses. AM wrote the manuscript with contributions from all co-authors. AM, AI, and AS provided grant and equipment support. All authors contributed to the article and approved the submitted version.

Conflict of interest

The authors declare that the research was conducted in the absence of any commercial or financial relationships that could be construed as a potential conflict of interest.

Publisher's note

All claims expressed in this article are solely those of the authors and do not necessarily represent those of their affiliated organizations, or those of the publisher, the editors and the reviewers. Any product that may be evaluated in this article, or claim that may be made by its manufacturer, is not guaranteed or endorsed by the publisher.

Supplementary material

The Supplementary Material for this article can be found online at: https://www.frontiersin.org/articles/10.3389/fmars.2023.1243713/full#supplementary-material

References

An, B., Li, T., Liu, J., Sun, H., and Chang, F. (2018). Spatial distribution and controlling factors of planktonic foraminifera in the modern western Pacific. *Quaternary Int.* 468, 14–23. doi: 10.1016/j.quaint.2018.01.003

Barrenechea Angeles, I., Lejzerowicz, F., Cordier, T., Scheplitz, J., Kucera, M., Ariztegui, D., et al. (2020). Planktonic foraminifera eDNA signature deposited on the seafloor remains preserved after burial in marine sediments. *Sci. Rep.* 10 (1), 1–12. doi: 10.1038/s41598-020-77179-8

Bé, A. W., and Anderson, O. R. (1976). Gametogenesis in planktonic foraminifera. *Science* 192 (4242), 890–892. doi: 10.1126/science.946914

Bé, A. W. H., and Tolderlund, D. S. (1971). "Distribution and ecology of living planktonic foraminifera in surface waters of the Atlantic and Indian oceans", in *The Micropaleontology of Oceans*, (Eds.) B. M. Funnel and W. R. Riedel (Cambridge: Cambridge University Press), pp. 105-149.

Bolyen, E., Rideout, J. R., Dillon, M. R., Bokulich, N. A., Abnet, C. C., Al-Ghalith, G. A., et al. (2019). Reproducible, interactive, scalable and extensible microbiome data science using QIIME 2. *Nat. Biotechnol.* 37, 852–857. doi: 10.1038/s41587-019-0209-9

Bouchet, V. M., Telford, R. J., Rygg, B., Oug, E., and Alve, E. (2018). Can benthic foraminifera serve as proxies for changes in benthic macrofaunal community structure? Implications for the definition of reference conditions. *Mar. Environ. Res.* 137, 24–36. doi: 10.1016/j.marenvres.2018.02.023

Camacho, C., Coulouris, G., Avagyan, V., Ma, N., Papadopoulos, J., Bealer, K., et al. (2009). BLAST+: architecture and applications. *BMC Bioinf.* 10, 1–9. doi: 10.1186/1471-2105-10-421

Cao, Y., Lei, Y., Fang, J. K. H., and Li, T. (2022). Molecular diversity of foraminiferal eDNA in sediments and their correlations with environmental factors from the Yellow Sea. *Ecol. Indic.* 142, 109294. doi: 10.1016/j.ecolind.2022.109294

Caromel, A. G., Schmidt, D. N., Phillips, J. C., and Rayfield, E. J. (2014). Hydrodynamic constraints on the evolution and ecology of planktic foraminifera. *Mar. Micropaleontol.* 106, 69–78. doi: 10.1016/j.marmicro.2014.01.002

Chaabane, S., de Garidel-Thoron, T., Giraud, X., Schiebel, R., Beaugrand, G., Brummer, G.-J., et al. (2023). The FORCIS database: A global census of planktonic Foraminifera from ocean waters. *Sci. Data* 10 (1), 354. doi: 10.1038/s41597-023-02264-2

Chao, A., Chiu, C.-H., and Jost, L. (2014). Unifying species diversity, phylogenetic diversity, functional diversity, and related similarity/differentiation measures through Hill numbers. *Annu. Rev. Ecol. Evol. System.* 45, 297–324. doi: 10.1146/annurev-ecolsys-120213-091540

Chao, A., and Jost, L. (2012). Coverage-based rarefaction and extrapolation: standardizing samples by completeness rather than size. *Ecology* 93 (12), 2533–2547. doi: 10.1890/11-1952.1

Chernihovsky, N., Torfstein, A., and Almogi-Labin, A. (2018). Seasonal flux patterns of planktonic foraminifera in a deep, oligotrophic, marginal sea: Sediment trap time series from the Gulf of Aqaba, northern Red Sea. *Deep Sea Res. Part I: Oceanogr. Res. Pap.* 140, 78–94. doi: 10.1016/j.dsr.2018.08.003

Cordier, T., Esling, P., Lejzerowicz, F., Visco, J., Ouadahi, A., Martins, C., et al. (2017). Predicting the ecological quality status of marine environments from eDNA metabarcoding data using supervised machine learning. *Environ. Sci. Technol.* 51 (16), 9118–9126. doi: 10.1021/acs.est.7b01518

Corliss, B. H. (1985). Microhabitats of benthic foraminifera within deep-sea sediments. *Nature* 314 (6010), 435–438. doi: 10.1038/314435a0

Darling, K. E., Kroon, D., Wade, C. M., and Leigh Brown, A. J. (1996). Molecular phylogeny of the foraminifera. *J. Foraminiferal Res.* 26 (4), 324–330. doi: 10.2113/gsjfr.26.4.324

Davis, C. V., Wishner, K., Renema, W., and Hull, P. M. (2021). Vertical distribution of planktic foraminifera through an oxygen minimum zone: how assemblages and test morphology reflect oxygen concentrations. *Biogeosciences* 18 (3), 977–992. doi: 10.5194/bg-18-977-2021

Deng, L., Bölsterli, D., Kristensen, E., Meile, C., Su, C. C., Bernasconi, S. M., et al. (2020). Macrofaunal control of microbial community structure in continental margin sediments. *Proc. Natl. Acad. Sci.* 117 (27), 15911–15922. doi: 10.1073/pnas.1917494117

Dimiza, M. D., Triantaphyllou, M. V., Koukousioura, O., Hallock, P., Simboura, N., Karageorgis, A. P., et al. (2016). The Foram Stress Index: A new tool for environmental assessment of soft-bottom environments using benthic foraminifera. A case study from the Saronikos Gulf, Greece, Eastern Mediterranean. *Ecol. Indic.* 60, 611–621. doi: 10.1016/j.ecolind.2015.07.030

Duffield, C. J., Edvardsen, B., Eikrem, W., and Alve, E. (2014). Effects of different potential food sources on upper-bathyal benthic foraminifera: an experiment with propagules. *J. Foraminiferal Res.* 44 (4), 416–433. doi: 10.2113/gsjfr.44.4.416

Enge, A. J., Nomaki, H., Ogawa, N. O., Witte, U., Moeseneder, M. M., Lavik, G., et al. (2011). Response of the benthic foraminiferal community to a simulated short-term phytodetritus pulse in the abyssal North Pacific. *Mar. Ecol. Prog. Ser.* 438, 129–142. doi: 10.3354/meps09298

Frontalini, F., Cordier, T., Balassi, E., du Chatelet, E. A., Cermakova, K., Apothéloz-Perret-Gentil, L., et al. (2020). Benthic foraminiferal metabarcoding and morphology-based assessment around three offshore gas platforms: Congruence and complementarity. *Environ. Int.* 144, 106049. doi: 10.1016/j.envint.2020.106049

Geslin, E., Heinz, P., Jorissen, F., and Hemleben, C. (2004). Migratory responses of deep-sea benthic foraminifera to variable oxygen conditions: laboratory investigations. *Mar. Micropaleontol.* 53 (3-4), 227–243. doi: 10.1016/j.marmicro.2004.05.010

Gollner, S., Kaiser, S., Menzel, L., Jones, D. O., Brown, A., Mestre, N. C., et al. (2017). Resilience of benthic deep-sea fauna to mining activities. *Mar. Environ. Res.* 129, 76–101. doi: 10.1016/j.marenvres.2017.04.010

Gooday, A. J. (1986). Meiofaunal foraminiferans from the bathyal Porcupine Seabight (northeast Atlantic): size structure, standing stock, taxonomic composition, species diversity and vertical distribution in the sediment. *Deep Sea Res. Part A. Oceanogr. Res. Pap.* 33 (10), 1345–1373. doi: 10.1016/0198-0149(86)90040-3

Gooday, A. J., Lejzerowicz, F., Goineau, A., Holzmann, M., Kamenskaya, O., Kitazato, H., et al. (2021). The biodiversity and distribution of abyssal benthic foraminifera and their possible ecological roles: A synthesis across the clarion-clipperton zone. *Front. Mar. Sci.* 8. doi: 10.3389/fmars.2021.634726

Gooday, A. J., Levin, L. A., Linke, P., and Heeger, T. (1992). "The Role of Benthic Foraminifera in Deep-Sea Food Webs and Carbon Cycling", in *Deep-Sea Food Chains and the Global Carbon Cycle. NATO ASI Series*, (eds) G. T. Rowe and V. Pariente (Dordrecht: Springer), vol 360. doi: 10.1007/978-94-011-2452-2_5

Holzmann, M., Hohenegger, J., Hallock, P., Piller, W. E., and Pawlowski, J. (2001). Molecular phylogeny of large miliolid foraminifera (Soritacea Ehrenberg 1839). *Mar. Micropaleontol.* 43 (1-2), 57–74. doi: 10.1016/S0377-8398(01)00021-4

Hothorn, T., and Hornik, K. (2022) *exactRankTests: Exact Distributions for Rank and Permutation Tests. R package version 0.8-35.* Available at: https://CRAN.R-project.org/package=exactRankTests.

Iguchi, A., Nishijima, M., Yoshioka, Y., Miyagi, A., Miwa, R., Tanaka, Y., et al. (2020). Deep-sea amphipods around cobalt-rich ferromanganese crusts: taxonomic diversity and selection of candidate species for connectivity analysis. *PloS One* 15, 1–11. doi: 10.1371/journal.pone.0228483

ISA. (2020). *ISA, International Seabed Authority Recommendations for the Guidance of Contractors for the Assessment of the Possible Environmental Impacts Arising from Exploration for Marine Minerals in the Area, ISBA/25/LTC/6/Rev.1.*

Jo, T., Murakami, H., Yamamoto, S., Masuda, R., and Minamoto, T. (2019). Effect of water temperature and fish biomass on environmental DNA shedding, degradation, and size distribution. *Ecol. Evol.* 9 (3), 1135–1146. doi: 10.1002/ece3.4802

Jones, D. O., Kaiser, S., Sweetman, A. K., Smith, C. R., Menot, L., Vink, A., et al. (2017). Biological responses to disturbance from simulated deep-sea polymetallic nodule mining. *PloS One* 12 (2), e0171750. doi: 10.1371/journal.pone.0171750

Jonkers, L., and Kučera, M. (2015). Global analysis of seasonality in the shell flux of extant planktonic Foraminifera. *Biogeosciences* 12 (7), 2207–2226. doi: 10.5194/bg-12-2207-2015

Jonkers, L., Reynolds, C. E., Richey, J., and Hall, I. R. (2015). Lunar periodicity in the shell flux of planktonic foraminifera in the Gulf of Mexico. *Biogeosciences* 12 (10), 3061–3070. doi: 10.5194/bg-12-3061-2015

Jorissen, F. J., de Stigter, H. C., and Widmark, J. G. (1995). A conceptual model explaining benthic foraminiferal microhabitats. *Mar. micropaleontol.* 26 (1-4), 3–15. doi: 10.1016/0377-8398(95)00047-X

Joseph, C., Faiq, M. E., Li, Z., and Chen, G. (2022). Persistence and degradation dynamics of eDNA affected by environmental factors in aquatic ecosystems. *Hydrobiologia* 849 (19), 4119–4133. doi: 10.1007/s10750-022-04959-w

Kawahata, H., Nishimura, A., and Gagan, M. K. (2002). Seasonal change in foraminiferal production in the western equatorial Pacific warm pool: evidence from sediment trap experiments. *Deep Sea Res. Part II: Topical Stud. Oceanogr.* 49 (13-14), 2783–2800. doi: 10.1016/S0967-0645(02)00058-9

Kvile, K. Ø., Taranto, G. H., Pitcher, T. J., and Morato, T. (2014). A global assessment of seamount ecosystems knowledge using an ecosystem evaluation framework. *Biol. Conserv.* 173, 108–120. doi: 10.1016/j.biocon.2013.10.002

Laroche, O., Kersten, O., Smith, C. R., and Goetze, E. (2020). Environmental DNA surveys detect distinct metazoan communities across abyssal plains and seamounts in the western Clarion Clipperton Zone. *Mol. Ecol.* 29 (23), 4588–4604. doi: 10.1111/mec.15484

Laroche, O., Wood, S. A., Tremblay, L. A., Ellis, J. I., Lear, G., and Pochon, X. (2018). A cross-taxa study using environmental DNA/RNA metabarcoding to measure biological impacts of offshore oil and gas drilling and production operations. *Mar. pollut. Bull.* 127, 97–107. doi: 10.1016/j.marpolbul.2017.11.042

Laroche, O., Wood, S. A., Tremblay, L. A., Ellis, J. I., Lejzerowicz, F., Pawlowski, J., et al. (2016). First evaluation of foraminiferal metabarcoding for monitoring environmental impact from an offshore oil drilling site. *Mar. Environ. Res.* 120, 225–235. doi: 10.1016/j.marenvres.2016.08.009

Lejzerowicz, F., Esling, P., and Pawlowski, J. (2014). Patchiness of deep-sea benthic Foraminifera across the Southern Ocean: Insights from high-throughput DNA sequencing. *Deep Sea Res. Part II: Topical Stud. Oceanogr.* 108, 17–26. doi: 10.1016/j.dsr2.2014.07.018

Lejzerowicz, F., Gooday, A. J., Barrenechea Angeles, I., Cordier, T., Morard, R., Apothéloz-Perret-Gentil, L., et al. (2021). Eukaryotic biodiversity and spatial patterns in the Clarion-Clipperton Zone and other abyssal regions: insights from sediment DNA and RNA metabarcoding. *Front. Mar. Sci.* 8, 671033. doi: 10.3389/fmars.2021.671033

Lessa, D., Morard, R., Jonkers, L., Venancio, I. M., Reuter, R., Baumeister, A., et al. (2020). Distribution of planktonic foraminifera in the subtropical South Atlantic: depth hierarchy of controlling factors. *Biogeosciences* 17 (16), 4313–4342. doi: 10.5194/bg-17-4313-2020

Li, Q., Lei, Y., Liu, J., Shen, Y., Huang, H., Wang, C., et al. (2022). Characteristics of foraminiferal communities in the western Clarion–Clipperton Zone revealed by eDNA metabarcoding. *J. Sea Res.* 189, 102286. doi: 10.1016/j.seares.2022.102286

Maechler, M., Rousseeuw, P., Struyf, A., Hubert, M., and Hornik, K. (2022). *cluster: Cluster Analysis Basics and Extensions. R package version 2.1.3.* Available at: https://CRAN.R-project.org/package=cluster.

Maeda, A., Kuroyanagi, A., Iguchi, A., Gaye, B., Rixen, T., Nishi, H., et al. (2022). Seasonal variation of fluxes of planktic foraminiferal tests collected by a time-series sediment trap in the central Bay of Bengal during three different years. *Deep Sea Res. Part I: Oceanogr. Res. Pap.* 183, 103718. doi: 10.1016/j.dsr.2022.103718

Meilland, M., Cornuault, P., Morard, R., Brummer, G.-J. A., and Kucera, M. (2022). Identification guide to extant planktonic foraminifera. Part 1: Family Candeinidae and genera Berggrenia, Bolivina, Dentigloborotalia, and Neogallitellia. *ICES Identification Leaflets Plankton* 196, 22. doi: 10.17895/ices.pub.7643

Milivojević, T., Rahman, S. N., Raposo, D., Siccha, M., Kucera, M., and Morard, R. (2021). High variability in SSU rDNA gene copy number among planktonic foraminifera revealed by single-cell qPCR. *ISME Commun.* 1 (1), 1–8. doi: 10.1038/s43705-021-00067-3

Moodley, L., Middelburg, J. J., Boschker, H. T., Duineveld, G. C., Pel, R., Herman, P. M., et al. (2002). Bacteria and Foraminifera: key players in a short term deep-sea benthic response to phytodetritus. *Mar. Ecol. Prog. Ser.* 236, 23–29. doi: 10.3354/meps236023

Morard, R., Lejzerowicz, F., Darling, K. F., Lecroq-Bennet, B., Winther Pedersen, M., Orlando, L., et al. (2017). Planktonic foraminifera-derived environmental DNA extracted from abyssal sediments preserves patterns of plankton macroecology. *Biogeosciences* 14 (11), 2741–2754. doi: 10.5194/bg-14-2741-2017

Morard, R., Vollmar, N. M., Greco, M., and Kucera, M. (2019). Unassigned diversity of planktonic foraminifera from environmental sequencing revealed as known but neglected species. *PloS One* 14 (3), e0213936. doi: 10.1371/journal.pone.0213936

Nozaki, T., Tokumaru, A., Takaya, Y., Kato, Y., Suzuki, K., and Urabe, T. (2016). Major and trace element compositions and resource potential of ferromanganese crust at Takuyo Daigo Seamount, northwestern Pacific Ocean. *Geochem. J.* 50 (6), 527–537. doi: 10.2343/geochemj.2.0430

Oksanen, J., Simpson, G. L., Blanchet, F. G., Kindt, R., Legendre, P., Minchin, P. R., et al. (2022). *vegan: Community Ecology Package. R package version 2.6-4.* Available at: https://github.com/vegandevs/vegan.

Orcutt, B. N., Bradley, J. A., Brazelton, W. J., Estes, E. R., Goordial, J. M., Huber, J. A., et al. (2020). Impacts of deep-sea mining on microbial ecosystem services. *Limnol. Oceanogr.* 65 (7), 1489–1510. doi: 10.1002/lno.11403

Ota, Y., Suzumura, M., Tsukasaki, A., Suzuki, A., Seike, K., and Minatoya, J. (2022). Sediment accumulation rates and particle mixing at northwestern Pacific seamounts. *J. Mar. Syst.* 229, 103719. doi: 10.1016/j.jmarsys.2022.103719

Patterson, R. T., and Fishbein, E. (1989). Re-examination of the statistical methods used to determine the number of point counts needed for micropaleontological quantitative research. *J. Paleontol.* 63 (2), 245–248. doi: 10.1017/S0022336000019272

Pawlowski, J., Bruce, K., Panksep, K., Aguirre, F. I., Amalfitano, S., Apothéloz-Perret-Gentil, L., et al. (2022). Environmental DNA metabarcoding for benthic monitoring: A review of sediment sampling and DNA extraction methods. *Sci. Total Environ.* 818, 151783. doi: 10.1016/j.scitotenv.2021.151783

Pawlowski, J., Esling, P., Lejzerowicz, F., Cedhagen, T., and Wilding, T. A. (2014). Environmental monitoring through protist next-generation sequencing metabarcoding: assessing the impact of fish farming on benthic foraminifera communities. *Mol. Ecol. Resour.* 14 (6), 1129–1140. doi: 10.1111/1755-0998.12261

Petro, C., Zäncker, B., Starnawski, P., Jochum, L. M., Ferdelman, T. G., Jørgensen, B. B., et al. (2019). Marine deep biosphere microbial communities assemble in near-surface sediments in Aarhus Bay. *Front. Microbiol.* 10, 758. doi: 10.3389/fmicb.2019.00758

Quast, C., Pruesse, E., Yilmaz, P., Gerken, J., Schweer, T., Yarza, P., et al. (2013). The SILVA ribosomal RNA gene database project: improved data processing and web-based tools. Opens external link in new window. *Nucl. Acids Res.* 41 (D1), D590–D596. doi: 10.1093/nar/gks1219

R Core Team (2021). *R: A language and environment for statistical computing* (Vienna, Austria: R Foundation for Statistical Computing). Available at: https://www.R-project.org/.

Roberts, D. W. (2019) *labdsv: Ordination and Multivariate Analysis for Ecology. R package version 2.0-1.* Available at: https://CRAN.R-project.org/package=labdsv.

Saito, T., and Doi, H. (2021). Degradation modeling of water environmental DNA: experiments on multiple DNA sources in pond and seawater. *Environ. DNA* 3 (4), 850–860. doi: 10.1002/edn3.192

Sansom, B. J., and Sassoubre, L. M. (2017). Environmental DNA (eDNA) shedding and decay rates to model freshwater mussel eDNA transport in a river. *Environ. Sci. Technol.* 51 (24), 14244–14253. doi: 10.1021/acs.est.7b05199

Sassoubre, L. M., Yamahara, K. M., Gardner, L. D., Block, B. A., and Boehm, A. B. (2016). Quantification of environmental DNA (eDNA) shedding and decay rates for three marine fish. *Environ. Sci. Technol.* 50 (19), 10456–10464. doi: 10.1021/acs.est.6b03114

Schiebel, R. (2002). Planktic foraminiferal sedimentation and the marine calcite budget. *Global Biogeochem. Cycles* 16 (4), 3–1. doi: 10.1029/2001GB001459

Schiebel, R., and Hemleben, C. (2017). Planktic foraminifers in the modern ocean. (Berlin, Heidelberg: Springer), 358. doi: 10.1007/978-3-662-50297-6

Seymour, M., Durance, I., Cosby, B. J., Ransom-Jones, E., Deiner, K., Ormerod, S. J., et al. (2018). Acidity promotes degradation of multi-species environmental DNA in lotic mesocosms. *Commun. Biol.* 1 (1), 4. doi: 10.1038/s42003-017-0005-3

Shi, J., Lei, Y., Li, H., and Li, T. (2021). NGS-metabarcoding revealing novel foraminiferal diversity in the Western Pacific Magellan Seamount sediments. *J. Oceanol. Limnol.* 39 (5), 1718–1729. doi: 10.1007/s00343-021-0427-0

Shi, J., Lei, Y., Li, Q., Lyu, M., and Li, T. (2020). Molecular diversity and spatial distribution of benthic foraminifera of the seamounts and adjacent abyssal plains in the tropical Western Pacific Ocean. *Mar. Micropaleontol.* 156, 101850. doi: 10.1016/j.marmicro.2020.101850

Storz, D., Schulz, H., Waniek, J. J., Schulz-Bull, D. E., and Kučera, M. (2009). Seasonal and interannual variability of the planktic foraminiferal flux in the vicinity of the Azores Current. *Deep Sea Res. Part I: Oceanogr. Res. Pap.* 56 (1), 107–124. doi: 10.1016/j.dsr.2008.08.009

Strickler, K. M., Fremier, A. K., and Goldberg, C. S. (2015). Quantifying effects of UV-B, temperature, and pH on eDNA degradation in aquatic microcosms. *Biol. Conserv.* 183, 85–92. doi: 10.1016/j.biocon.2014.11.038

Teal, L. R., Bulling, M. T., Parker, E. R., and Solan, M. (2008). Global patterns of bioturbation intensity and mixed depth of marine soft sediments. *Aquat. Biol.* 2 (3), 207–218. doi: 10.3354/ab00052

Toro, N., Galvez, E., Saldana, M., and Jeldres, R. I. (2022). Submarine mineral resources: A potential solution to political conflicts and global warming. *Minerals Eng.* 179, 107441. doi: 10.1016/j.mineng.2022.107441

Usui, A., Nishi, K., Sato, H., Nakasato, Y., Thornton, B., Kashiwabara, T., et al. (2017). Continuous growth of hydrogenetic ferromanganese crusts since 17 Myr ago on Takuyo-Daigo Seamount, NW Pacific, at water depths of 800–5500 m. *Ore Geol. Rev.* 87, 71–87. doi: 10.1016/j.oregeorev.2016.09.032

Walker, M., Hammel, J. U., Wilde, F., Hoehfurtner, T., Humphries, S., and Schuech, R. (2021). Estimation of sinking velocity using free-falling dynamically scaled models: Foraminifera as a test case. *J. Exp. Biol.* 224 (2), jeb230961. doi: 10.1242/jeb.230961

Watling, L., and Auster, P. J. (2021). Vulnerable marine ecosystems, communities, and indicator species: Confusing concepts for conservation of seamounts. *Front. Mar. Sci.* 8, 622586. doi: 10.3389/fmars.2021.622586

Weber, A. A., and Pawlowski, J. (2013). Can abundance of protists be inferred from sequence data: a case study of Foraminifera. *PloS One* 8 (2), e56739. doi: 10.1371/journal.pone.0056739

Weinkauf, M. F., Siccha, M., and Weiner, A. K. (2022). Reproduction dynamics of planktonic microbial eukaryotes in the open ocean. *J. R. Soc. Interface* 19 (187), 2021. doi: 10.1098/rsif.2021.0860

Wickham, H. (2016). *ggplot2: Elegant Graphics for Data Analysis* (New York: Springer-Verlag).

Yamasaki, M., Sasaki, A., Oda, M., and Domitsu, H. (2008). Western equatorial Pacific planktic foraminiferal fluxes and assemblages during a La Niña year, (1999). *Mar. Micropaleontol.* 66 (3-4), 304–319. doi: 10.1016/j.marmicro.2007.10.006